Food and Bioprocess Technology (2018) 11:1516–1526
https://doi.org/10.1007/s11947-018-2122-5

Mass Transfer Kinetic and Quality Changes During High-Pressure Impregnation (HPI) of Jumbo Squid (*Dosidicus gigas*) Slices

Roberto Lemus-Mondaca[1] · Carlos Zambra[2] · Fernanda Marín[3] · Mario Pérez-Won[4] · Gipsy Tabilo-Munizaga[4]

Received: 19 June 2017 / Accepted: 23 May 2018 / Published online: 2 June 2018
© Springer Science+Business Media, LLC, part of Springer Nature 2018

Abstract

Jumbo squid is an important marine resource commercialized in Chile as well as American countries such as Perú, México, and USA. In order to find the best conditions for prevention of squid meat degradation, this study presented the simultaneous application of high hydrostatic pressure and osmotic dehydration (high-pressure impregnation (HPI)) on jumbo squid (*Dosidicus gigas*) slices. Diffusion coefficients for both components water and solids are improved by the high-pressure processing. The pressures used were 100, 250, and 400 MPa for a 15 g/100 mL salt concentration for time intervals of 30 s. The mathematical expressions used for mass transfer simulations of both water and salt were those corresponding to Newton, Henderson and Pabis, Page, and Weibull models, where the Weibull model presented the best fitted to the experimental data for both components. As to quality parameters studied for texture profile analysis, the treatment at 250 MPa yielded on the samples a minimum hardness, whereas springiness, cohesiveness, and chewiness at 100-, 250-, and 400-MPa treatments presented statistical differences regarding unpressurized samples. The color parameters L^* (lightness) increased; however, b^* (yellowish) and a^* (reddish) parameters decreased when increasing pressure level. This way, samples presented a brighter aspect and a mildly cooked appearance. The results presented in this study could support the potential of high hydrostatic pressure application as a technique novel for other compound impregnation under high pressure.

Keywords Jumbo squid · Osmotic dehydration · High pressure · Process modeling · Color changes · Texture profile

Introduction

The jumbo squid (*Dosidicus gigas*) is the largest invertebrate of the pelagic seacoast fauna as well as specie more important in Chilean waters (Fernández and Vásquez 1995; Rocha and Vega 2003). In recent years, jumbo squid has become a resource of great relevance in the fishing industry of Chile that is why external demand has increased in landings, development, and commercialization of this resource (Ibáñez and Ulloa 2014). Usually, jumbo squid is marketed as fresh or frozen product and among their nutritional properties includes its high protein content and low fat content (Abugoch et al. 1999).

As a way to minimize physical, chemical, and biological reactions leading to a deterioration of fresh seafood, the necessity arises to develop new processing techniques in the fishing industry (Valencia-Pérez et al. 2008). Osmotic dehydration (OD) is a mass transfer mechanism in which water is partially removed from foods by immersing them in hypertonic solutions such as syrup or brine (Uribe et al. 2011). Furthermore, this technology is used as a pretreatment to improve nutritional, sensorial, and functional properties of food without changing its integrity. During this process, the cell membrane acts as a semi-permeable film; two main fluxes, namely, the diffusion of water out of the tissue into the osmotic solution due to osmosis and the uptake of solute from osmotic solution to the product, happen in a simultaneous and opposite mode (Lemus-Mondaca et al. 2009). Among the benefits of OD is that it reduces the moisture content and thus convert it to intermediate moisture food, helping to increase

✉ Roberto Lemus-Mondaca
rlemus@uchile.cl

✉ Carlos Zambra
czambra@utalca.cl

[1] Departamento de Ciencia de los Alimentos y Tecnología Química, Facultad de Ciencias Químicas y Farmacéuticas, Universidad de Chile, Santos Dumont 964, Independencia, Santiago, Chile

[2] Departamento de Tecnologías Industriales, Facultad de Ingeniería, Universidad de Talca, Camino Los Niches Km 1, Curicó, Chile

[3] Departamento de Ingeniería en Alimentos, Universidad de La Serena, Av. Raúl Bitrán 1305, La Serena, Chile

[4] Departamento de Ingeniería en Alimentos, Universidad del Bío-Bío, Av. Andrés Bello 720, Chillán, Chile

the shelf life of the product (Chavan et al. 2010). As a way to describe the mass transfer phenomena during the OD of foodstuffs, some authors have used empirical mathematical models while others have used the analytical unsteady solution of Fick's law second to estimate diffusion coefficients of water loss and solid uptake. However, information that is available in literature regarding these models on the simulation of OD of jumbo squid are limited (Uribe et al. 2011).

In literature, it is reported that the high-pressure treatment under intervals between 100 and 700 MPa and 200–400 MPa enhanced the water and solid diffusion for OD of pineapples (Rastogi and Niranjan 1998) and strawberries (Nuñez-Mancilla et al. 2011), respectively. Similarly, Villacís et al. (2008) showed that high-pressure processing affected component diffusion into turkey breast. They found that moisture diffusion coefficient infusing out of the sample was minimum at 150 MPa, whereas NaCl diffusion coefficient infusing into the sample was maximum at 150 MPa. Also, Zhang et al. (2015) investigated the effect of HP processing under single and two cycles on physicochemical and microbial properties of squid (*Todarodes pacificus*) pieces during 4 °C storage. These researchers demonstrated that the two-cycle HP treatment was more effective in controlling microbial growth and quality deterioration regarding the single-cycle treatment, thus more desirable for extending shelf life of fresh squids. Other studies have been applying high hydrostatic pressure in different food such as marine and vegetables products (Briones-Labarca et al. 2012; Landl et al. 2010), which focused on microbiological and physicochemical characteristics.

To our knowledge, no research has been performed on the effect of high hydrostatic pressure on the osmotic dehydration kinetics and quality aspects of jumbo squid. In this way, the aim of this research was to study and model the mass transfer kinetics of moisture and solids during simultaneous osmotic dehydration and high hydrostatic pressure on jumbo squid at different pressures and to assess their effect on quality aspects such as color and analysis profile textural.

Materials and Methods

Raw Material and High-Pressure Impregnation

Jumbo squid (*D. gigas*) was obtained at the local fish market at the seaport of Coquimbo, Chile. Jumbo squid were cleaned, washed, and chopped into slices of 5.0 ± 0.2 cm each side and 1.0 ± 0.1-cm thickness, and then were maintained refrigerated at 4.0 ± 0.2 °C. The osmotic solutions were prepared using commercial salt and distilled water. Then, samples were weighed individually and submerged in the hypertonic solution (NaCl, 15 g/100 mL) in a 1/8 (*w*/*w*) jumbo squid to water ratio and packaged in polyethylene bags prior to high-pressure impregnation (HPI) processing. HPI treatment was carried out in a cylindrical loading container at 15 °C in a 2-L pilot high-pressure unit (Avure Technologies Inc., Kent, WA, USA). Water was employed as the pressurizing medium, working at 17 MPa/s ramp rate; decompression time was less than 5 s. Samples were subjected to three different high-pressure conditions, 100, 250, and 400 MPa along with a control treatment (unpressurized samples) at atmospheric pressure, 0.1 MPa. The measurements were performed at 30-s intervals until reaching 300 s (final time). The samples treated were removed from the hypertonic solution after HPI treatment, and the excess of saline solution on the surface was eliminated with tissue paper. Then, moisture and salt content in the samples impregnated was determined following the method of A.O.A.C. 934.06, while salt content was determined by the Mohr method (A.O.A.C. 1990). Each experiment was carried out in triplicate.

Determination of Water and Solid Diffusion Coefficients

Mass transfer kinetics during treatment HPI has been modeled using Fick's second law of diffusion (Chenlo et al. 2007). In this model, the dependent variable is the moisture ratio (MR) or solid ratio (SR) which relate the mass transfer gradient (moisture and solid) in real time to both initial and equilibrium contents (moisture and solid; Eq. 1) (Uribe et al. 2011). Considering the jumbo squid as semi-infinite slice with initially uniform water and solid contents, the solution for Fick's equation for constant process conditions is (Crank 1975)

$$MR\_or\_SR = \sum_{i=0}^{\infty} \frac{8}{(2i+1)\pi^2} \exp\left(\frac{D_e(2i+1)\pi^2 t}{4L^2}\right) \quad (1)$$

This way, the variables of this model diffusional are moisture loss (MR; Eq. 2) and salt gain rate (SR; Eq. 3) (Uribe et al. 2011), represented as follows:

$$MR = \frac{M_t}{M_o} = \frac{8}{\pi^2} \exp\left(\frac{D_{we}\pi^2 t}{4L^2}\right) \quad (2)$$

$$SR = \frac{S_t}{S_o} = \frac{8}{\pi^2} \exp\left(\frac{D_{se}\pi^2 t}{4L^2}\right) \quad (3)$$

where MR and SR are the moisture and salt ratios, respectively; M_t and S_t are the moisture or solid contents in real time, respectively; M_o and S_o are the initial moisture content or solids, respectively; D_{we} and D_{se} are the effective diffusivity of water or solid (m^2/s); t is the process time (min); and L is the half-thickness of the slice (m).

Mathematical Models

Mathematical modeling of mass transfer selection of mathematical models was based on those previously proposed in agricultural products during osmotic dehydration and can also be found on previous works (Corzo and Bracho 2008; Vega-Gálvez et al. 2011; Uribe et al. 2011). The selected mathematical models are

$$\text{Newton} \quad MR\_or\_SR = \exp(-k_1 t) \tag{4}$$

$$\text{Henderson-Pabis} \quad MR\_or\_SR = a\exp(-k_2 t) \tag{5}$$

$$\text{Page} \quad MR\_or\_SR = \exp(-k_3 t^n) \tag{6}$$

$$\text{Weibull} \quad MR\_or\_SR = \exp\lfloor -(t/\beta)^{\alpha} \rfloor \tag{7}$$

Statistical Evaluation of Models

The determination coefficient (R^2), sum squared error (*SSE*; Eq. 8), root mean square error (RMSE; Eq. 9), and chi-squared (χ^2; Eq. 10) statistical tests values were applied; these were selected as optimal criteria in order to evaluate the fit quality of the empirical models, and then to select the equation which best described the osmotic dehydration curves.

$$SSE = \frac{1}{N}\sum_{i=0}^{N}\left(MR_{ei}\_or\_SR_{\mathrm{ei}} - MR_{ci}\_or\_SR_{ci}\right)^2 \tag{8}$$

$$RMSE = \left[\frac{1}{N}\sum_{i=0}^{N}\left(MR_{ci}\_or\_SR_{ci} - MR_{ei}\_or\_SR_{ei}\right)^2\right]^{1/2} \tag{9}$$

$$\chi^2 = \frac{\sum_{i=0}^{N}\left(MR_{ei}\_or\_SR_{\mathrm{ei}} - MR_{ci}\_or\_SR_{ci}\right)^2}{N-z} \tag{10}$$

where MR_{ei} is the moisture content experimental, MR_{ci} is the calculated moisture content, i is the number of terms, z is a constant number, and N is the number of data.

Quality Parameters

Proximal Analysis

The moisture content was determined following the method of A.O.A.C. 934.06, using an analytical balance (CHYO, Jex-120, Kyoto, Japan) with an accuracy of ± 0.0001 g and a vacuum drying oven at 50 °C (Gallenkamp, OVA–031, Leicester, UK). The crude protein content was determined using the Kjeldahl method with a conversion factor of 6.25 (A.O.A.C. 960.52). The lipid content was analyzed gravimetrically following Soxhlet extraction (A.O.A.C. 960.39). The crude ash content was estimated by incineration in a muffle furnace (Felisa, FE-341, Jalisco, Mexico) at 550 °C (A.O.A.C. 923.03). Finally, the salt content of the samples was determined by the Mohr method (A.O.A.C. 1990). All the analyses mentioned above were performed in triplicate and expressed in g/100 g dry matter.

Measurement of Textural Characteristics

The instrumental texture profile analysis (TPA) of jumbo squid samples was carried out with a texture analyzer (Model TA-TX PLUS, Texture Technologies, Scarsdale, NY, USA). The sample was compressed to 75% of its original thickness with speed of 1 mm/s; the samples were compressed twice. Texture analysis was automatically performed by the texture expert software (v.2.63; Stable Micro Systems Ltd.), and the following parameters were recorded: hardness (N), maximum force required to compress the sample; cohesiveness (dimensionless), extent to which the sample could be deformed prior to rupture; springiness (cm), ability of sample to recover its original form after the deforming force is removed; and chewiness (N/cm), the work needed to chew a solid sample at a steady state of swallowing (Bourne et al. 1966). Ten replicated instrumental measurements were performed for each analysis.

Surface Color

Evaluation of color changes in the surface of the samples was done using a colorimeter (HunterLab, model MiniScan XE Plus, Reston, VA, USA), including an opening 2.5-cm diameter where light goes through. The measurements were expressed by Hunter Lab units L^*, a^*, and b^* values which represent light-dark spectrum with a range from 0 (black) to 100 (white), the green-red spectrum with a range from − 60 (green) to + 60 (red), and the blue-yellow spectrum with a range from − 60 (blue) to + 60 (yellow) dimensions, respectively, along with a standard illuminant D_{65} and Observer 10° (Vega-Gálvez et al. 2011). The colorimeter yielded L^*, a^*, and b^* values for each spot, which were converted to the total value of color difference (ΔE) according to Eq. 10. The experiments were done in triplicate.

$$\Delta E = \sqrt{\Delta L^{*2} + \Delta a^{*2} + \Delta b^{*2}} \tag{11}$$

Statistical Analysis of Quality Parameters

Statistical analysis of experimental data was determined using Statgraphics Plus® v.5.1 software (STSC, Inc. 1991), applying an analysis of variance (ANOVA) to estimate any statistically significant differences at a confidence level of 95% ($P < 0.05$) along with a multiple range test (MRT) for the comparison of data.

Results and Discussion

Mass Transfer Kinetics and Diffusion Coefficients

Proximate analysis of jumbo squid presented an initial moisture content of 88.31 ± 0.69 g, crude protein (N × 6.25) of 18.42 ± 0.80 g, total lipids of 0.10 ± 0.01 g, ash of 1.06 ± 0.04 g, and salt content of 1.92 ± 0.01 g, where all results obtained were expressed in 100 g dry matter. Similar results were reported by Abugoch et al. (1999), Cortés-Ruiz et al. (2008), Uribe et al. (2011), and Vega-Gálvez et al. (2011).

Figure 1 shows the changes in the experimental profiles of moisture and salt contents during HPI (100–400 MPa) of jumbo squid. During this process, simultaneous water and salt movement occurred. As a result, the properties of the muscle were also modified. Water and salt transfer rate into jumbo squid took place, owing to the differences in osmotic concentration and pressure gradient between muscle cells and the salting agent. Water content decreased while salt content increased with an increase in pressure from 100 to 400 MPa. Focusing on Fig. 1b, it shows a plot of SR vs. pressurizing time where the SR at 400 MPa is above 100 MPa. The same pattern repeats over the whole process time. Therefore, SR, which stands for salt ratio, increases with pressure. Likewise, lower values of water content and higher salt contents in comparison to the unpressurized samples (0.1 MPa) were obtained. The variation in these values is likely due to HPI-induced modifications of the cell wall structure (primarily the non-covalent bonds) leaving the cells more permeable and resulting in increased mass transfer rate (Landl et al. 2010).

To compare the mass transfer characteristics, both water and solute diffusion coefficient into the sample were calculated. Table 1 shows water and salt diffusion coefficients during HPI under 100, 250, and 400 MPa, which varied from 14.18–20.26 and 1.62–4.05 × 10^{-9} m^2/s, respectively. The water and salt diffusivities from pressurized samples were always higher than diffusivities of the unpressurized samples; the higher values for water and salt diffusivity were observed to 100 MPa. These values decreased with increasing the pressure level to 400 MPa ($P < 0.05$). This observed effect could be attributed to the changes in the cell structure due to high-pressure application (Villacís et al. 2008). Previous reports on meat products (meat, pork, turkey, chicken among other) showed that the increase in NaCl content with pressure treatment up 150 MPa resulted in increased water-holding capacity since the increase in ionic strength due to NaCl diffusion solubilized the muscle protein, which in turn resulted in higher water-holding capacity and tenderness (Gou et al. 2003; Villacís et al. 2008). Pressures above 150 MPa resulted in decrease in solubility of protein (Macfarlane and McKenzie 1976), and complete denaturation was obtained at 300 MPa (Ikkai and Ooi 1966). Villacís et al. (2008) reported that water and salt diffusion coefficient decreased and increased, respectively, up to 150 MPa; further increase in pressure to 300 MPa resulted that moisture diffusivity increased and NaCl diffusivity decreased for turkey breast samples. Sopanangkul et al. (2002) reported that the sucrose diffusion coefficient in

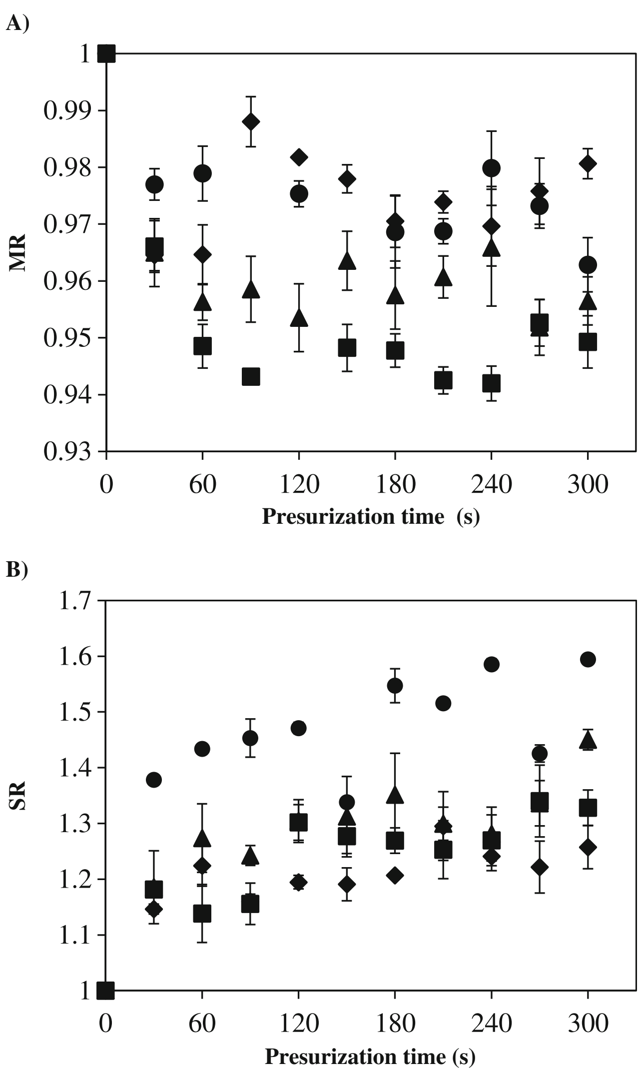

Fig. 1 **a** Water loss and **b** solid gain during HPI of jumbo squid samples at different pressures: 0.1 MPa (black diamond), 100 MPa (black square), 250 MPa (black triangle), and 400 MPa (black circle). Values are the mean ± standard deviation of triplicate

Table 1 Diffusion coefficients of solids (D_s) and water (D_w) and at different operating pressures

Pressure (MPa)	$D_w \times 10^{-9}$ (m^2/s)	$D_s \times 10^{-9}$ (m^2/s)
0.1	1.62 ± 0.11 a	14.18 ± 2.86 a
100	8.11 ± 0.28 c	36.47 ± 5.73 b
250	8.10 ± 0.55 c	31.07 ± 2.33 c
400	4.05 ± 0.21 b	20.26 ± 1.40 d

Different letters in the same column indicate significant differences ($P <$ 0.05). All values are the mean ± standard deviation of triplicate potato cylinders increased significantly under high pressure. Uribe et al. (2011) reported that the diffusion coefficients for water and salt increased with temperature (75–95 °C) during osmotic dehydration of jumbo squid samples. Nuñez-Mancilla et al. (2011) working with simultaneous application of high hydrostatic pressure during osmotic dehydration of strawberries observed that diffusion coefficients for moisture and soluble solids are improved by increasing the pressure (200–400 MPa).

Diffusion coefficient values reported in literature have been difficult to compare because of the different estimation methods and models employed along with the variation in food composition, physical structure, and processing conditions (Azoubel and Murr 2004). As mentioned above, this phenomenon could be explained by species diversity, process temperatures and pressures, concentration of osmotic agent, muscle orientation, fat content, and presence or absence of skin, among other (Gallart-Jornet et al. 2007).

Mathematical Modeling of Experimental Curves

Several mathematical models were selected to simulate the HPI process of jumbo squid. Table 2 shows the empirical parameter values for each mathematical model of both MR and SR. It can be seen that the parameter values for MR, k_1 (Newton), k_2 (Henderson-Pabis), and k_3 (Page), presented a clear tendency to decrease as pressure increased; however, the a parameter (Henderson-Pabis) showed an opposite behavior ($P < 0.05$). Weibull model and n parameter Page did not show a clear pattern with respect to process ($P < 0.05$). Regarding parameter values for solid transfer, most of the kinetic parameters increased their values when pressure was increased during osmotic dehydration; however, the n parameter of Page and α parameter of Weibull did not show a clear pattern with pressure, e.g., Newton (k_1), Henderson-Pabis (k_2), and Page (k_3). Parameters showed a clear growing tendency with pressure ($P < 0.05$). That is why it may be assumed that these empirical parameters would be directly proportional at working pressure. In the literature, there is insufficient data on mathematical modeling of osmotic dehydration of jumbo squid during high hydrostatic pressure. Nevertheless, Nuñez-Mancilla et al. (2011) presented similar results for osmotic dehydration of strawberries under high pressure to apply the Newton, Henderson-Pabis, and Page models on SR regarding this study, while that moisture content showed opposite behavior. Uribe et al. (2011) reported that this model did not show a clear pattern with respect to process temperature when mathematical modeling was used to study the effect of process temperature (85 and 95 °C) on moisture and salt mass transfer during osmotic dehydration of jumbo squid. Pérez-Won et al. (2016) found that Weibull parameters could be directly proportional to brine osmotic concentration in the study simultaneous application of osmotic dehydration and high pressure as a pretreatment to drying process on red abalone.

Statistical Analysis of Models

The results of statistical tests performed to the proposed models are shown in Table 3; the value tests were in the range of 0.0001–0.0009 for SSE, 0.0048–0.0312 for RMSE, and 0.0001–0.0011 for χ^2 for moisture and in the range of 0.0037–0.2343 for SSE, 0.0173–0.4841 for RMSE, and

Table 2 Model parameters for moisture (MR) and solid (SR) transfer during HPI of jumbo squid at different pressures

Model	Parameters		Pressures (MPa)			
			0.1	100	250	400
Newton	k_1	MR	0.003 ± 0.000 a	0.015 ± 0.001 d	0.0106 ± 0.0019 c	0.008 ± 0.000 b
		SR	0.047 ± 0.003 a	0.058 ± 0.012 ab	0.068 ± 0.004 b	0.097 ± 0.006 c
Henderson-Pabis	k_2	MR	0.003 ± 0.000 a	0.015 ± 0.001 d	0.0106 ± 0.0019 c	0.008 ± 0.000 b
		SR	0.047 ± 0.003 a	0.058 ± 0.012 ab	0.068 ± 0.004 b	0.097 ± 0.006 c
	A	MR	0.998 ± 0.001 a	0.993 ± 0.001 c	0.995 ± 0.001 bc	0.997 ± 0.001 ab
		SR	1.036 ± 0.013 a	1.041 ± 0.024 a	1.041 ± 0.024 a	1.044 ± 0.003 a
Page	k_3	MR	0.032 ± 0.001 ab	0.038 ± 0.000 b	0.035 ± 0.003 ab	0.025 ± 0.002 a
		SR	0.148 ± 0.006 a	0.145 ± 0.023 a	0.205 ± 0.026 b	0.357 ± 0.006 c
	n	MR	0.865 ± 0.155 a	0.263 ± 0.054 b	0.136 ± 0.012 b	0.313 ± 0.022 b
		SR	0.302 ± 0.004 ab	0.456 ± 0.018 c	0.329 ± 0.004 bc	0.163 ± 0.003 a
Weibull	α	MR	0.865 ± 0.155 a	0.263 ± 0.054 b	0.136 ± 0.012 b	0.313 ± 0.022 b
		SR	0.302 ± 0.004 ab	0.456 ± 0.018 c	0.329 ± 0.004 bc	0.163 ± 0.003 a
	β	MR	62.625 ± 6.410 a	120.96 ± 8.844 b	752.76 ± 33.396 c	373.01 ± 26.341 d
		SR	568.796 ± 126.545 a	70.387 ± 12.793 b	153.768 ± 6.939 b	583.381 ± 6.587 a

Different letters (a, b, c, d) in the same line indicate significant differences ($P < 0.05$). All values are the mean ± standard deviation of triplicate

Table 3 Statistical test performed for each mathematical model regarding moisture loss and solid gain

Model		Test	Pressure (MPa)			
			0.1	100	250	400
Newton	MR	R^2	0.9403	0.9077	0.9251	0.9063
		SSE	0.0009	0.0003	0.0003	0.0004
		RMSE	0.0312	0.0196	0.0182	0.0222
		χ^2	0.0011	0.0004	0.0004	0.0006
	SR	R^2	0.8788	0.9452	0.9244	0.8909
		SSE	0.0146	0.0210	0.0251	0.0418
		RMSE	0.2211	0.2449	0.2585	0.2046
		χ^2	0.0479	0.0356	0.0507	0.0512
Henderson-Pabis	MR	R^2	0.9403	0.9077	0.9251	0.9463
		SSE	0.0008	0.0004	0.0002	0.0003
		RMSE	0.0293	0.0205	0.0157	0.0199
		χ^2	0.0010	0.0005	0.0003	0.0004
	SR	R^2	0.8788	0.9452	0.9244	0.8909
		SSE	0.1556	0.0134	0.0184	0.0326
		RMSE	0.3945	0.2160	0.1356	0.1806
		χ^2	0.1902	0.0164	0.0224	0.0398
Page	MR	R^2	0.9295	0.9491	0.9077	0.9403
		SSE	0.0007	0.0001	0.0002	0.0001
		RMSE	0.0277	0.0116	0.0048	0.0119
		χ^2	0.0009	0.0001	0.0002	0.0001
	SR	R^2	0.8284	0.9350	0.9616	0.9466
		SSE	0.2343	0.0337	0.0223	0.0797
		RMSE	0.4841	0.1937	0.1496	0.2824
		χ^2	0.0412	0.0414	0.0573	0.0874
Weibull	MR	R^2	0.9295	0.9491	0.9077	0.9403
		SSE	0.0007	0.0001	0.0002	0.0001
		RMSE	0.0277	0.0116	0.0048	0.0119
		χ^2	0.0009	0.0001	0.0002	0.0001
	SR	R^2	0.8284	0.9350	0.9616	0.9466
		SSE	0.0299	0.0038	0.0037	0.0079
		RMSE	0.0173	0.0184	0.0192	0.0282
		χ^2	0.0031	0.0046	0.0045	0.077

0.0045–0.1902 for χ^2 for solids. From these results, the equation that described impregnation kinetics of jumbo squid data due to the high values of R^2 and less values of the SSE and χ^2 was Weibull model for both components. Therefore, for good fit, this mathematical model could be applied adequately for predicting the high-pressure impregnation effects of jumbo squid, which is necessary for design, optimization, and process efficiency. From Fig. 2, a comparison to experimental and estimated mass transfer profiles using the Weibull model can be observed. In literature, similar results were reported by other authors when simulating osmotic dehydration of strawberries, where the Weibull model gave the best goodness of fit on the experimental data (Nuñez-Mancilla et al. 2011). Also, the same Weibull model was the most suitable to describe the mass transfer phenomena during osmotic dehydration of jumbo squid (Uribe et al. 2011); likewise, Corzo and Bracho (2008) reported that Weibull model adequately predicted the moisture and salt contents of sardine sheets during vacuum pulse (10 min) osmotic dehydration at brine concentration 0.15–0.27 g NaCl/g and 30–38 °C. Cunha et al. (2001) found that the Weibull model described the water loss kinetics in apple during osmotic dehydration in sucrose solutions at five levels for sucrose concentration (0.45 ± 0.65 *w/w*) and temperature (20 ± 40 °C).

Modification of Texture Induced by HHP

The TPA results are summarized in Table 4, where the effect of high-pressure impregnation on the hardness, springiness, cohesiveness, and chewiness parameters can be observed. The hardness, springiness, cohesiveness, and chewiness values of the control sample were 1977 ± 621, 0.70 ± 0.12, 0.58 ± 0.14, and 909 ± 435, respectively. In this case, hardness indicates the firmness of jumbo squid sample, the cohesiveness indicates the stickiness, springiness indicates the elasticity, and chewiness indicates the tenderness of the jumbo squid muscle (Briones-Labarca et al. 2012). As to the experimental values, these presented changes significantly in the hardness, springiness, cohesiveness, and chewiness, showing a tendency to increase with increasing applied pressure ($P < 0.05$).

For hardness, smaller values were observed for the samples pressurized at 250 MPa, and higher values were presented at 400 MPa. A similar behavior was described by Chéret et al. (2005), who observed an increase proportional to the increase in pressure, above 300 MPa, allowing the hardness of fillets to stay in a good range for consumers who reject soft fish flesh. Also, Ashie and Simpson (1996) reported for bluefish samples a direct tendency regarding texture under pressure from 100 to 300 MPa. Ma and Ledward (2004) informed that structural alterations in the contractile myofibrillar proteins were the main factor responsible for texture changes. Rastogi et al. (2007) performed an experiment under a pressure range from 100 to 300 MPa. They established for this range pressure that the changes are normally reversible, whereas higher pressures normally are non-reversible. Lamballerie-Anton et al. (2002) researched the lysosomes rupture at pressures around 200 MPa, promoting an increase in autolytic activity and tenderization of the meat.

The effect of high pressure on springiness, cohesiveness, and chewiness was slight, where the samples treated at 400 MPa showed a tendency to increase these values. Similar values were reported by Chéret et al. (2005) on sea bass fillets (day 0), where the hardness increases with increasing pressure from 100 to 500 MPa; however, these showed a decrease to 200-MPa treatment, while cohesiveness and springiness were almost constant, and chewiness decreased

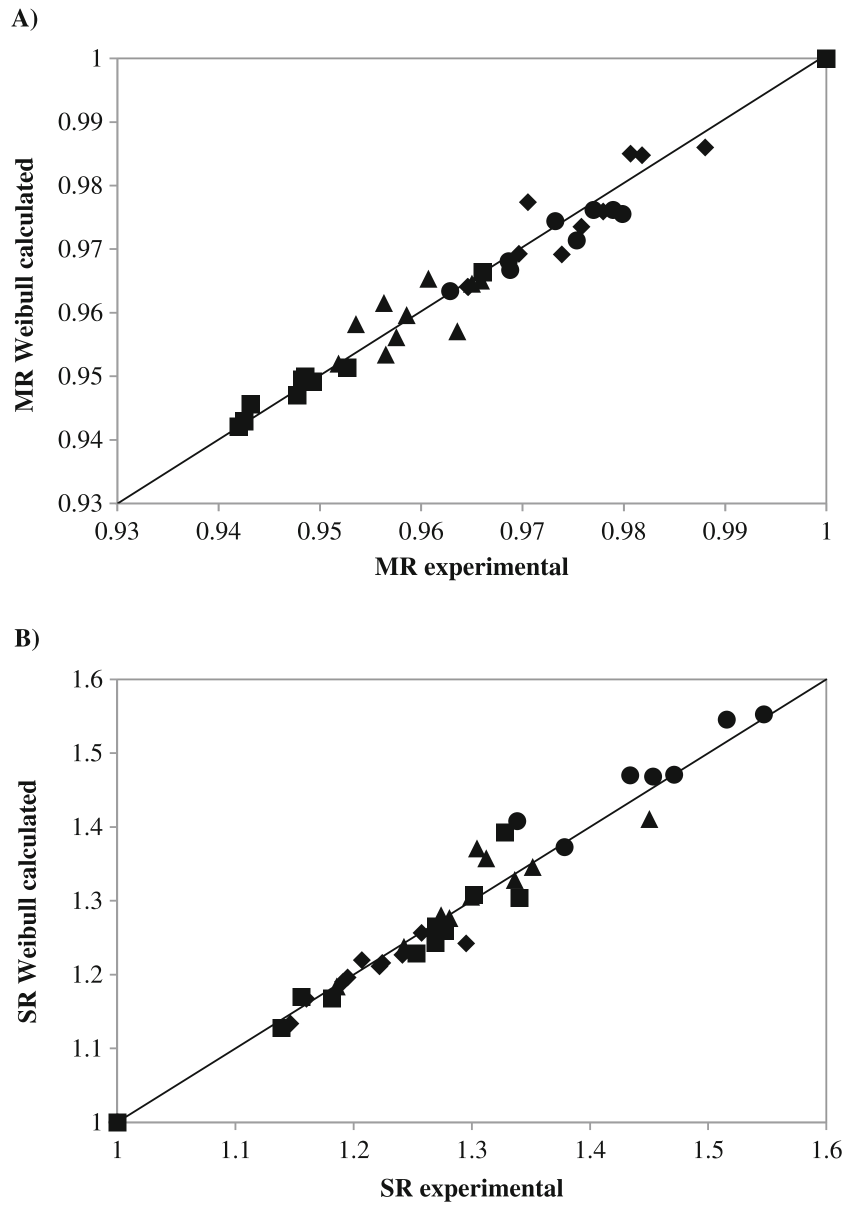

Fig. 2 Comparison between experimental and estimated values. **a** Water loss and **b** solid gain during HPI of jumbo squid samples at different pressures: 0.1 MPa (black diamond), 100 MPa (black square), 250 MPa (black triangle), and 400 MPa (black circle)

from 100 to 300 MPa and increased after 400-MPa treatment. Villacís et al. (2008) studied the HHP effect on turkey breast muscles treated above 150 MPa. They measured hardness, cohesiveness, and chewiness, where these values increased with increasing pressure; similarly, Angsupanich and Ledward (1998) reported that cod muscle (*Gadus morhua*) showed an increase in springiness when they were submitted to pressures of 400 and 600 MPa for 20 min. Yagiz et al. (2007) looked into the effect of high pressure on rainbow trout; in this case, the cohesiveness values were significantly higher in samples subjected to pressures between 300 and 600 MPa. However, Ashie et al. (1997) reported that pressurization at 100 MPa induced an increase in hardness (strength/firmness) in bluefish muscle, whereas at higher pressures (from 200 to 300 MPa), this parameter seemed to decrease. In the case of carp muscle, Yoshioka and Yamamoto (1998) observed a softening for all the studied pressure range (100–500 MPa), with a minor increase in hardness by increasing pressure. The effects of high pressure on fish texture ensue from these modifications of the water bond, protease activity, aggregation or gelation of myosin, and sarcoplasmic proteins (Angsupanich and Ledward 1998).

Color Evolution

Table 5 shows the evolution of lightness (L^*), red/green (a^*), and yellow/blue (b^*) coordinates related to pressure and impregnation time. The chromatic coordinate values for the control samples L^*, a^*, and b^* were 74.82 ± 0.02, −4.09 ± 0.02, and 3.31 ± 0.05, respectively. L^* values of jumbo squid

Table 4 Texture profile analysis parameters of jumbo squid samples treated by high-pressure impregnation

Pressurization time (s)	0.1 MPa	100 MPa	250 MPa	400 MPa
Hardness (gf)				
30	1928 ± 592 b	1227 ± 56 ab	879 ± 364 b	1502 ± 1479 ab
60	2329 ± 629 a	1857 ± 1001 c	1610 ± 632 b	2468 ± 365 a
90	2150 ± 300 a	1513 ± 250 b	689 ± 195 a	1676 ± 447 a
120	2126 ± 450 a	2347 ± 1861 a	1288 ± 295 b	2617 ± 689 a
150	2746 ± 142 a	1942 ± 673 b	808 ± 180 a	2032 ± 678 a
180	2589 ± 532 a	1723 ± 638 b	1674 ± 676 a	1930 ± 568 a
210	1592 ± 253 a	2285 ± 897 a	642 ± 152 a	2407 ± 1130 b
240	1379 ± 419 a	2453 ± 653 a	1211 ± 537 a	2904 ± 1152 b
270	1587 ± 227 a	1390 ± 578 b	1231 ± 559 a	1989 ± 615 a
300	1164 ± 148 a	1089 ± 734 a	953 ± 136 a	4123 ± 2004 b
Springiness (mm)				
30	0.78 ± 0.10 a	0.66 ± 0.11 b	0.79 ± 0.07 b	0.71 ± 0.08 a
60	0.74 ± 0.05 a	0.76 ± 0.06 c	0.72 ± 0.07 b	0.81 ± 0.04 a
90	0.77 ± 0.09 a	0.70 ± 0.15 b	0.69 ± 0.13 b	0.82 ± 0.04 a
120	0.70 ± 0.05 a	0.55 ± 0.09 b	0.72 ± 0.06 a	0.78 ± 0.10 c
150	0.75 ± 0.07 a	0.75 ± 0.09 c	0.67 ± 0.06 b	0.77 ± 0.05 a
180	0.74 ± 0.03 a	0.53 ± 0.11 b	0.76 ± 0.05 c	0.79 ± 0.03 a
210	0.77 ± 0.06 a	0.82 ± 0.06 b	0.67 ± 0.12 b	0.73 ± 0.06 a
240	0.78 ± 0.05 a	0.85 ± 0.03 c	0.73 ± 0.13 b	0.82 ± 0.06 a
270	0.79 ± 0.05 a	0.63 ± 0.08 b	0.73 ± 0.06 b	0.80 ± 0.05 a
300	0.77 ± 0.04 a	0.75 ± 0.08 c	0.69 ± 0.05 b	0.80 ± 0.03 a
Cohesiveness				
30	0.53 ± 0.06 a	0.68 ± 0.07 b	0.65 ± 0.14 b	0.52 ± 0.09 b
60	0.60 ± 0.06 a	0.52 ± 0.10 b	0.66 ± 0.16 bc	0.63 ± 0.09 c
90	0.46 ± 0.08 a	0.63 ± 0.08 c	0.45 ± 0.12 b	0.66 ± 0.07 bc
120	0.46 ± 0.07 a	0.37 ± 0.09 b	0.75 ± 0.10 d	0.59 ± 0.09 c
150	0.47 ± 0.05 a	0.48 ± 0.10 b	0.40 ± 0.07 b	0.65 ± 0.07 c
180	0.48 ± 0.04 a	0.31 ± 0.09 c	0.57 ± 0.06 c	0.68 ± 0.15 b
210	0.51 ± 0.11 a	0.67 ± 0.10 c	0.40 ± 0.09 b	0.67 ± 0.08 c
240	0.57 ± 0.06 a	0.68 ± 0.10 c	0.58 ± 0.17 b	0.70 ± 0.04 bc
270	0.60 ± 0.05 a	0.41 ± 0.10 b	0.59 ± 0.08 c	0.68 ± 0.08 c
300	0.53 ± 0.06 a	0.65 ± 0.07 c	0.50 ± 0.08 b	0.69 ± 0.09 bc
Chewiness (mm)				
30	586 ± 116 a	1638 ± 354 c	329 ± 207 b	405 ± 213 ab
60	1524 ± 264 a	168 ± 65 b	304 ± 153 a	536 ± 279 a
90	869 ± 158 a	220 ± 181 b	197 ± 92 a	1290 ± 662 a
120	1026 ± 227 a	160 ± 79 b	240 ± 204 a	1286 ± 347 a
150	1482 ± 502 a	318 ± 88 b	223 ± 75 a	1210 ± 220 a
180	1137 ± 86 a	182 ± 87 b	480 ± 287 a	852 ± 273 a
210	514 ± 41 a	2098 ± 656 b	188 ± 51 ^{a}	1376 ± 612 ^{a}
240	1124 ± 66 a	1569 ± 478 b	356 ± 105 ^{a}	1788 ± 653 ^{a}
270	592 ± 61 a	249 ± 157 b	348 ± 148 ^{a}	1247 ± 210 ^{a}
300	638 ± 179 a	263 ± 133 b	278 ± 87 a	312 ± 91 a

Different letters (a, b, c, d) in the same row indicate significant differences ($P < 0.05$). All values are the mean ± standard deviation of 10 values

samples increased with increasing treatment pressure ($P < 0.05$). Samples treated at 100 MPa showed the lowest L^* values and treatment at 400 MPa resulted in the highest L^* values, which were significantly ($P < 0.05$) higher than

Table 5 Effect of high hydrostatic pressure to different time conditions on color (ΔE) and chromatic coordinates L^*, a^*, and b^* of fresh and pressurized jumbo squid samples

Pressurization time	Pressure (MPa)	Chromatic coordinates			
		L^*	a^*	b^*	ΔE
30 s	0.1	63.18 ± 0.13 a	− 4.76 ± 0.05 a	− 1.86 ± 0.25 a	12.75 ± 0.15 a
	100	63.79 ± 0.14 b	− 4.22 ± 0.06 c	0.09 ± 0.01 c	1.96 ± 0.10 c
	250	63.86 ± 0.16 b	− 4.35 ± 0.01 b	− 1.98 ± 0.02 a	1.69 ± 0.11 d
	400	69.05 ± 0.08 c	− 4.78 ± 0.02 a	− 4.54 ± 0.10 b	4.70 ± 0.07 b
60 s	0.1	67.39 ± 0.30 a	− 5.24 ± 0.15 a	− 0.53 ± 0.04 a	8.02 ± 0.15 a
	100	62.73 ± 0.42 b	− 4.55 ± 0.05 c	1.30 ± 0.01 c	2.57 ± 0.01 d
	250	67.58 ± 0.14 a	− 4.69 ± 0.02 bc	− 0.17 ± 0.08 a	5.08 ± 0.15 c
	400	70.98 ± 0.66 c	− 4.79 ± 0.03 b	− 4.05 ± 0.39 b	5.75 ± 0.29 b
90 s	0.1	65.98 ± 0.32 a	− 4.97 ± 0.03 a	− 1.41 ± 0.10 a	10.96 ± 0.33 a
	100	63.64 ± 0.12 c	− 4.52 ± 0.04 c	3.34 ± 0.28 c	4.68 ± 0.24 c
	250	64.91 ± 0.24 b	− 4.53 ± 0.05 c	− 1.25 ± 0.06 a	2.38 ± 0.23 d
	400	71.16 ± 0.12 d	− 4.83 ± 0.03 b	− 3.26 ± 0.07 b	5.47 ± 0.07 b
120 s	0.1	62.58 ± 0.16 a	− 4.97 ± 0.02 a	− 1.26 ± 0.04 a	13.09 ± 0.16 a
	100	64.79 ± 0.12 b	− 4.35 ± 0.02 c	0.90 ± 0.05 d	3.11 ± 0.10 d
	250	66.64 ± 0.13 c	− 4.48 ± 0.10 b	− 0.75 ± 0.04 c	4.10 ± 0.14 c
	400	72.02 ± 0.17 d	− 4.99 ± 0.02 a	− 3.90 ± 0.22 b	6.55 ± 0.04 b
150 s	0.1	65.41 ± 0.14 a	− 4.80 ± 0.05 a	− 0.22 ± 0.02 a	9.93 ± 0.13 a
	100	64.32 ± 0.10 b	− 4.25 ± 0.03 d	1.37 ± 0.07 c	3.20 ± 0.09 d
	250	66.90 ± 0.50 c	− 4.39 ± 0.08 c	− 2.81 ± 0.28 b	4.65 ± 0.38 c
	400	71.42 ± 0.06 d	− 5.29 ± 0.05 b	− 2.93 ± 0.28 b	5.62 ± 0.13 b
180 s	0.1	66.01 ± 0.67 a	− 4.84 ± 0.06 a	− 1.07 ± 0.07 a	9.87 ± 0.58 a
	100	61.50 ± 0.60 b	− 4.20 ± 0.06 c	1.43 ± 0.04 d	3.04 ± 0.20 d
	250	66.25 ± 0.25 a	− 4.65 ± 0.02 b	− 1.94 ± 0.07 b	3.74 ± 0.24 c
	400	72.14 ± 0.34 c	− 4.78 ± 0.03 a	− 3.75 ± 0.04 c	6.56 ± 0.29 b
210 s	0.1	68.56 ± 0.80 a	− 4.53 ± 0.05 a	− 2.02 ± 0.06 a	8.24 ± 0.64 a
	100	65.33 ± 0.47 c	− 3.90 ± 0.02 d	0.75 ± 0.03 d	3.56 ± 0.39 d
	250	67.36 ± 0.37 b	− 4.34 ± 0.08 c	− 1.03 ± 0.01 c	4.80 ± 0.38 c
	400	72.27 ± 0.06 d	− 4.98 ± 0.03 b	− 3.37 ± 0.13 b	6.53 ± 0.03 b
240 s	0.1	65.32 ± 0.30 a	− 4.88 ± 0.04 a	− 2.28 ± 0.06 a	11.05 ± 0.23 a
	100	66.69 ± 0.37 b	− 4.23 ± 0.01 d	0.46 ± 0.02 d	4.48 ± 0.33 c
	250	66.94 ± 0.32 b	− 4.31 ± 0.03 c	− 1.34 ± 0.15 c	4.40 ± 0.32 c
	400	73.29 ± 0.15 c	− 4.82 ± 0.02 b	− 2.64 ± 0.08 b	7.23 ± 0.15 b
270 s	0.1	63.49 ± 0.65 a	− 4.82 ± 0.10 a	− 1.96 ± 0.11 a	12.52 ± 0.58 a
	100	62.76 ± 0.20 a	− 4.41 ± 0.05 c	0.33 ± 0.02 d	1.70 ± 0.04 c
	250	68.49 ± 1.26 b	− 4.01 ± 0.05 d	− 0.78 ± 0.03 c	6.08 ± 1.21 b
	400	72.47 ± 0.08 c	− 5.2 ± 0.05 b	− 2.69 ± 0.07 b	6.50 ± 0.06 b
300 s	0.1	64.31 ± 0.23 a	− 4.72 ± 0.05 a	− 2.30 ± 0.15 a	11.93 ± 0.28 a
	100	66.56 ± 0.31 b	− 4.23 ± 0.06 d	1.04 ± 0.03 d	4.62 ± 0.26 d
	250	68.49 ± 0.37 c	− 4.39 ± 0.03 c	− 2.62 ± 0.11 b	6.09 ± 0.35 c
	400	73.85 ± 0.21 d	− 4.60 ± 0.03 b	− 1.98 ± 0.19 c	7.63 ± 0.24 b

Different letters (a, b, c, d) in the same column indicate significant differences ($P < 0.05$). All values are the mean ± standard deviation of triplicate

unpressurized samples. This might indicate that high-pressure treatment produced a brighter and less transparent appearance on jumbo squid tissue (Cruz-Romero et al. 2007). The protein coagulation changes sample surface properties, increases light reflection, and results in white color (Kruk et al. 2011). The muscle has an appearance as cooked, and this effect was accentuated with an increase in pressure. The increase in lightness of samples by higher pressures was might be due to protein coagulation and loss of active pigments. These results were similar to those observed in turbot fillets (Chevalier et al. 2001) and oysters (Cruz-Romero et al. 2004).

The a^* values for samples decreased with increasing pressure. Significant changes in a^* values of samples for all pressure treatments applied ($P < 0.05$) were found. These changes may be linked to denaturation of the myofibrillar and sarcoplasmic proteins (Ma and Ledward 2004). Angsupanich and Ledward (1998) reported similar changes in color for cod treated at 100–200 MPa, where myosin was denatured under these pressures. Furthermore, Chéret et al. (2005) and Cruz-Romero et al. (2004) found similar values in HP-treated sea bass fillets and HP-treated oysters, respectively. The yellow/blue color indicator (b^*) showed the highest values in samples treated at 100 MPa, while samples treated at 400 MPa obtained the lowest values ($P < 0.05$). In addition, ΔE values of samples are a good indicator of progressive changes in color of treated samples by high hydrostatic pressure. Statistical analysis of the ΔE values, as indicator of total color difference, showed that there were significant increases ($P < 0.05$) with increasing treatment pressure 100 to 400 MPa; however, these values were lower at 0.1-MPa values. Lipid oxidation is one cause of color loss in fish products due to degradation of highly unsaturated carotenoids such as astaxanthin, one of the major pigments in shellfish and fish products. Cruz-Romero et al. (2007) reported that ΔE values of 3.0–6.0, 6.0–12.0, and > 12 correspond to very distinctive, strong, and very strong differences, and according to this scale, high-pressure-treated samples exhibit very distinct while than unpressurized very strong color differences.

Conclusion

This investigation demonstrated that application of high hydrostatic pressure from 100 to 400 MPa influences the mass transfer phenomena during osmotic dehydration of jumbo squid immersed in saline solution. The HPI treatment enhanced the water and salt diffusion coefficients in comparison to unpressurised samples (0.1 MPa); specifically, pressurized samples showed a twofold increase in salt diffusion coefficient. According to the statistical analysis, the model that best describes the experimental impregnation kinetics was Weibull model due to the presentation of the best-fit statistical tests performed. Thus, this model may be applied to simulate the mass transfer during HPI of jumbo squid. HPI treatment influenced quality of jumbo squid in term of hardness, springiness, cohesiveness, and chewiness of the samples; these parameters were affected by applied pressure level. Pressure at 250 MPa showed a minimum hardness while for springiness, cohesiveness, and chewiness treatments of 100, 250, and 400 MPa presented statistical differences regarding unpressurized samples. The same happened for color results, where changes were also observed in chromatic coordinates due to increasing pressure that led to a noticeable modification of surface sample, giving cooked appearance. Finally, the results present here provide further support for the potential of hydrostatic pressure application as a novel and promising impregnation technique that can be used to improve food sensory acceptance, enhancing product quality and reducing process times.

Funding Information The authors gratefully acknowledge the financial support provided by FONDECYT Regular No. 1140067 Project and DIULS Tesis Postgrado PT15331 project for publication of this research.

References

A.O.A.C. (1990). *Official method of analysis (15th ed)*. Washington: Association of Official Analytical Chemists.

Abugoch, L., Guarda, A., Perez, L., & Paredes, M. (1999). Determination of proximal chemical composition of squid (*Dosidicus gigas*) and development of a gel product. *Archivos Latinoamericanos de Nutrición, 49*(2), 156–161.

Angsupanich, K., & Ledward, D. A. (1998). High pressure treatment effects on cod (*Gadus morhua*) muscle. *Food Chemistry, 63*(1), 39–50.

Ashie, I. N. A., & Simpson, B. K. (1996). Application of high hydrostatic pressure to control enzyme related fresh seafood texture deterioration. *Food Research International, 29*(5-6), 569–575.

Ashie, I. N. A., Simpson, B. K., & Ramaswamy, H. S. (1997). Changes in texture and microstructure of pressure-treated fish muscle tissue during chilled storage. *Journal of Muscle Foods, 8*(1), 13–32.

Azoubel, P. M., & Murr, F. E. X. (2004). Mass transfer kinetic of osmotic dehydration of cherry tomato. *Journal of Food Engineering, 61*, 291–295.

Bourne, M. C., Moyer, J. C., & Hand, D. B. (1966). Measurement of food texture by a universal testing machine. *Food Technology, 20*, 522–552.

Briones-Labarca, V., Perez-Won, M., Zamarca, M., Aguilera-Radic, J. M., & Tabilo-Munizaga, G. (2012). Effects of high hydrostatic pressure on microstructure, texture, color and biochemical changes of red abalone (*Haliotis rufecens*) during cold storage time. *Innovative Food Science and Emerging Technologies, 13*, 42–50.

Chavan, U. D., Prabhukhanolkar, A. E., & Pawar, V. D. (2010). Preparation of osmotic dehydrated ripe banana slices. *Journal of Food Science and Technology, 47*(4), 380–386.

Chenlo, F., Moreira, C., Fernández-Herrero, C., & Vázquez, G. (2007). Mass transfer during osmotic dehydration of chestnut using sodium chloride solutions. *Journal of Food Engineering, 73*, 164–173.

Chéret R, Chapleau, N., Delbarre-Ladrat C, Verrez-Bagnis V., and De Lamballerie-Anton M. (2005). Effects of high pressure on texture and microstructure of sea bass (*Dicentrarchus labrax* L.) fillets. Journal of Food Science, 70(8), 477–483.

Chevalier, D., Bail, A. L., & Ghoul, M. (2001). Effects of high pressure treatment (100–200 MPa) at low temperature on turbot (*Scophthalmus maximus*) muscle. *Food Research International, 34*(5), 425–429.

Cortés-Ruiz, J., Pacheco-Aguilar, R., Lugo-Sanchez, M., Carvallo-Ruiz, M., & Garcia-Sanchez, G. (2008). Production and functional evaluation of a protein concentrate from giant squid (*Dosidicus gigas*) by acid dissolution and isoelectric precipitation. *Food Chemistry, 110*(2), 486–492.

Corzo, O., & Bracho, N. (2008). Application of Weibull distribution model to describe the vacuum pulse osmotic dehydration of sardine sheets. *LWT Food Science and Technology, 41*(6), 1108–1115.

Crank, J. (1975). *The mathematics of diffusion* (2nd ed.). London: Oxford University Press.

Cruz-Romero, M., Smiddy, M., Hill, C., Kerry, J. P., & Kelly, A. L. (2004). Effects of high-pressure treatment on physicochemical characteristics of fresh oysters (*Crassostrea gigas*). *Innovative Food Science and Emerging Technologies, 5*(2), 161–169.

Cruz-Romero, M., Kelly, A. L., & Kerry, J. P. (2007). Effects of high-pressure and heat treatments on physical and biochemical characteristics of oysters (*Crassostrea gigas*). *Innovative Food Science and Emerging Technologies, 8*(1), 30–38.

Cunha, L. M., Oliveira, F. A. R., Aboim, A. P., & Frías, J. M. (2001). Stochastic approach to the modeling of water losses during osmotic dehydration and improved parameter estimation. *International Journal of Food Science and Technology, 36*, 253–262.

Fernández, F., & Vásquez, J. (1995). La Jibia gigante *Dosidicus gigas* (Orbigny 1835) en Chile: Análisis de una pesquera efímera. *Estudios Oceanológicos, 14*, 17–21.

Gallart-Jornet, L., Barat, J. M., Rustad, T., Erikson, U., Escriche, I., & Fito, P. (2007). Influence of brine concentrations on Atlantic salmon fillet salting. *Journal of Food Engineering, 80*(1), 267–275.

Gou, P., Comaposada, J., & Arnau, J. (2003). NaCl content and temperature effects on moisture diffusivity in the Gluteus medius muscle of pork ham. *Meat Science, 63*(1), 29–34.

Ibáñez, C. M., & Ulloa, P. (2014). Desarrollo de la pesquería y comercialización del calamar *Dosidicus gigas* en Chile. Desarrollo de la pesquería y comercialización del calamar *Dosidicus gigas* (Cephalopoda, Ommastrephidae) en Chile. *Amici Molluscarum, 22*, 7–14.

Ikkai, T., & Ooi, T. (1966). The effects of pressure on F-G transformation of actin. *Biochemistry, 5*(5), 1551–1560.

Kruk, Z. A., Yun, H., Rutley, D. L., Lee, E. J., Kim, Y. J., & Jo, C. (2011). The effect of high pressure on microbial population, meat quality and sensory characteristics of chicken breast fillet. *Food Control, 22*(1), 6–12.

Lamballerie-Anton, M. D., Taylor, R. G., & Culioli, J. (2002). High pressure processing of meat. In J. Kerry, J. Kerry, & D. Ledward (Eds.), *Meat processing: improving quality* (pp. 313–324). Cambridge: Woodhead Publishing Limited.

Landl, A., Abadias, M., Sárraga, C., Viñas, I., & Picouet, A. P. (2010). Effect of high pressure processing on the quality of acidified Granny Smith apple purée product. *Innovative Food Science and Emerging Technologies, 11*, 557–564.

Lemus-Mondaca, R., Miranda, M., Ándres, A., Briones, V., Villalobos, R., & Vega-Gálvez, A. (2009). Effect of osmotic pretreatment on hot-air drying kinetics and quality of Chilean papaya (*Carica pubescens*). *Drying Technology, 27*(10), 1105–1115.

Ma, H. J., & Ledward, D. A. (2004). High pressure/thermal treatment effects on the texture of beef muscle. *Meat Science, 68*(3), 347–355.

Macfarlane, J. J., & McKenzie, I. J. (1976). Pressure induced solubilization of myofibrillar proteins. *Journal of Food Science, 41*(6), 1442–1446.

Nuñez-Mancilla, Y., Perez-Won, M., Vega-Gálvez, A., Arias, V., Tabilo-Munizaga, G., & Briones-Labarca, V. (2011). Modeling mass transfer during osmotic dehydration of strawberries under high hydrostatic pressure conditions. *Innovative Food Science and Emerging Technologies, 12*(3), 338–343.

Pérez-Won, M., Lemus-Mondaca, R., Tabilo-Munizaga, G., Pizarro, S., Noma, S., Igura, N., & Shimoda, M. (2016). Modelling of red abalone (*Haliotis rufescens*) slices drying process: Effect of osmotic dehydration under high pressure as a pretreatment. *Innovative Food Science and Emerging Technologies, 34*, 127–134.

Rastogi, N. K., and Niranjan, K. (1998). Enhanced mass transfer during osmotic dehydration of high pressure treated pineapple. Journal of Food Science, 63, 3–5, 508, 511.

Rastogi, N. K., Raghavarao, K. S., Balasubramaniam, V. M., Niranjan, K., & Knorr, D. (2007). Opportunities and challenges in high pressure processing of foods. *Critical Review in Food Science and Nutrition, 47*(1), 69–112.

Rocha, F., & Vega, M. (2003). Overview of cephalopod fisheries in Chilean waters. *Fisheries Research, 60*(1), 151–159.

Sopanangkul, A., Ledward, D. A., & Niranjan, K. (2002). Mass transfer during sucrose infusion into potatoes under high pressure. *Journal of Food Science, 67*(6), 2217–2220.

STSC, Inc. (1991). Statgraphics statistical graphics system, Version 51. Rockville, Md: STSC, Inc.

Uribe, E., Miranda, M., Vega-Gálvez, A., Quispe, I., Clavería, R., & Di Scala, K. (2011). Mass transfer modelling during osmotic dehydration of jumbo squid (*Dosidicus gigas*): influence of temperature on diffusion coefficients and kinetic parameters. *Food Bioprocess Technology, 4*(2), 320–326.

Valencia-Pérez, A., García-Morales, M., Cárdenas-López, J., Herrera-Urbina, J., Rouzaud-Sández, O., & Ezquerra-Brauer, J. (2008). Effect of thermal process on connective tissue from jumbo squid (*Dosidicus gigas*) mantle. *Food Chemistry, 107*(4), 1371–1378.

Vega-Gálvez, A., Miranda, M., Clavería, R., Quispe, I., Vergara, J., Uribe, E., Paez, H., & Di Scala, K. (2011). Effect of air temperature on drying kinetics and quality characteristics of osmo-treated jumbo squid (*Dosidicus gigas*). *LWT-Food Science and Technology, 44*(1), 16–23.

Villacís, M. F., Rastogi, N. K., & Balasubramaniam, V. M. (2008). Effect of high pressure on moisture and NaCl diffusion into turkey breast. *LWT-Food and Science Technology, 41*(5), 836–844.

Yagiz, Y., Kristinsson, H. G., Balaban, M. O., & Marshall, M. R. (2007). Effect of high pressure treatment on the quality of rainbow trout (*Oncorhynchus mykiss*) and mahi mahi (*Coryphaena hippurus*). *Food Chemistry and Toxicology, 72*(9), 509–515.

Yoshioka, K., & Yamamoto, T. (1998). Changes of ultrastructure and the physical properties of carp muscle by high pressurization. *Fisheries Science, 64*(1), 89–94.

Zhang, Y., Jiao, S., Lian, Z., Deng, Y., & Zhao, Y. (2015). Effect of single- and two-cycle high hydrostatic pressure treatments on water properties, physicochemical and microbial qualities of minimally processed squids (*Todarodes pacificus*). *Journal of Food Science, 80*(5), E1012–E1020.